Propagation of Viruses on Micropatterned Host Cells

Elizabeth E. Endler,[1] Karen A. Duca,[1,2] Paul F. Nealey,[1] George M. Whitesides,[3] John Yin[1]

[1]Department of Chemical Engineering, University of Wisconsin–Madison, 1415 Engineering Drive, Madison, Wisconsin 53706-1691 telephone: 608-265-3779; fax: 608-262-5434; e-mail: yin@engr.wisc.edu
[2]Department of Electrical Engineering and Computer Science, Tufts University, Medford, Massachusetts 02153
[3]Department of Chemistry and Chemical Biology, Harvard University, Cambridge, Massachusetts 02138

Received 21 May 2002; accepted 7 August 2002

DOI: 10.1002/bit.10516

Abstract: We have developed a technique to characterize the in vitro propagation of viruses. Microcontact printing was used to generate linear arrays of alkanethiols on gold surfaces, which served as substrates for the patterned culture of baby hamster kidney (BHK-21) cells. Vesicular stomatitis virus (VSV) was added to unpatterned cell reservoirs adjacent to the patterned cells and incubated, setting in motion a continuously advancing viral infection into the patterned cells. At different incubation times, multiple arrays were chemically fixed to stop the viral propagation. Viral propagation distances into the patterned cells were determined by indirect immunofluorescent labeling and visualization of the VSV surface glycoprotein (G). The infection spread at approximately 50 μm/h in the 140-μm lines. Moreover, different temporal stages of the infection process were simultaneously visualized along individual lines. These stages included initiation of infection, based on G protein expression; cell–cell fusion, based on virus-induced clustering of cell nuclei; and cytoskeletal degradation, based on localized release of cells from the surface. This work sets a foundation for parallel, high-throughput characterization of viral and cellular processes. *Biotechnol Bioeng* **81**: 719–725, 2003.
Keywords: micropatterned cells; viral characterization; self-assembled monolayer

INTRODUCTION

During the last century, the development of plaque assays has facilitated the study of viruses that infect plant (Beijerinck, 1898), bacterial (d'Herelle, 1917; Twort, 1915), and animal (Dulbecco, 1952) hosts. Initially, these assays revealed the particulate nature of viruses and provided a reliable means to measure their infectious titer. The assay is performed by applying a dilute solution of viruses to a monolayer of susceptible host cells. Each virus particle adsorbs to a cell and initiates a spreading infection that eventually becomes visible to the unaided eye as a "plaque," or an island of dying or dead cells surrounded by a sea of uninfected cells. By counting the plaques and knowing the volume and dilution of solution added, one can calculate the concentration of infectious particles in the original solution. As a useful byproduct of the assay, the relative sizes, shapes, and turbidities of plaques have historically served to classify virus mutants (Block et al., 1993; Cooper, 1961; Dallo et al., 1987; Gong et al., 1989; Iizuka et al., 1989). Furthermore, because the virus progeny within a plaque have descended from a single virus particle, single plaques provide a useful source of genetically pure virus (Sambrook et al., 1989). Alternatively, if a plaque is cultured for an extended period of time, mutant viruses may emerge, and the plaque can provide an opportunity to study the evolutionary dynamics of virus populations descended from a single virion Lee and Yin, 1996; Yin, 1993).

In addition to genetic and evolutionary information, we envision that plaque-based methods of virus culture and characterization will also eventually furnish data-rich reports on the in vitro dynamics of viral infections. Three limitations, however, must be overcome. First, it is not clear to what extent the intracellular kinetics of the numerous reactions involved in infectious processes can be extracted from the observable plaque size, plaque morphology, or plaque expansion rate. Although it may be known in specific cases why the plaque of a mutant virus grows faster or to a larger size than that of a wild-type virus, it is not yet known how differences in mechanisms or rates of intracellular reactions quantitatively influence plaque sizes. Second, plaque sizes and expansion rates only provide information on cytopathic effect (CPE), or cell death, a relatively late stage of the virus–cell interaction. They reveal no information on earlier stages such as the dynamics of innate cellular responses to infection, or the production of viral mRNAs, proteins, genomes, or progeny viruses. Third, the cell culture environment is often poorly defined. Although progress has been made toward understanding how cell culture conditions, including the presence of serum in culture

Correspondence to: J. Yin
Contract grant sponsor: Whitaker Foundation; Merck Research Laboratories; National Science Foundation
Contract grant number: BES-0087939

media, affect cell growth and proliferation (Iyer et al., 1999; Terramani et al., 2000), and how agarose gel overlays restrict the free diffusion of virus particles (Duca et al., 2001), experiments are typically performed on tissue culture polystyrene (TCPS), a material with a surface chemistry that is heterogeneous (Steele et al., 1995). The nature of the interaction between living cells and the surfaces to which they adhere can have wide-reaching effects on the cell physiology or degree of differentiation (Chen et al., 1997, 1998; Dike et al., 1999; Franco et al., 2000; Healy et al., 1996; Lewandowska et al., 1992). Therefore, in vitro surface chemistries can indirectly or directly influence virus–cell interactions.

These challenges are not insurmountable, and initial progress is being made on all fronts. To address the first point, mathematical modeling of the processes involved in viral infection has provided a framework around which to begin to understand the connection between intracellular viral growth, mechanisms of cell-to-cell transport of viruses, and observed propagation rates (Yin and McCaskill, 1992; You and Yin, 1999). On the second point, viral and host components present during various stages in a spreading infection have been labeled using immunocytochemistry and visualized with fluorescence microscopy, revealing early events that occur well ahead of visible CPE (Duca et al., 2001). This methodology has revealed dramatically different host responses to viral infection that were not visible by the traditional plaque assay. However, this assay was performed in multiwell tissue culture polystyrene plates, giving the researcher little means of controlling surface chemistry or cell geometry. Finally, to begin to address the third point, we show here how cell-patterning methods using self-assembled monolayers to create well-defined cell positions may enhance our ability to control and monitor propagating viral infections.

Self-assembled monolayers (SAMs) provide a means to control the molecular composition of cell culture substrates and, therefore, a means to influence cell adhesion (Ostuni et al., 1999). Alkanethiols on gold surfaces are a versatile class of SAMs, and they can be patterned easily by a variety of methods. Microcontact printing has gained popularity for patterning cell culture substrates because it is a flexible, reproducible method for generating molecularly defined regions in a variety of shapes with dimensions ranging <1 μm to >100 μm (Kane et al., 1999). This methodology has been especially useful for identifying extracellular cues that regulate growth, differentiation, or apoptosis in cells (Chen et al., 1997, 1998; Dike et al., 1999).

As a model system, we studied vesicular stomatitis virus (VSV) propagation in linear arrays of baby hamster kidney (BHK-21) cells. VSV is well characterized (Rose and Whitt, 2001), has a wide host range, grows readily in culture, and induces clear CPE in many cell lines. Furthermore, commercially available antibodies to the surface glycoprotein of VSV enable monitoring of viral protein production via immunofluorescent labeling. In this study we demonstrate a method to control and characterize the in vitro propagation of VSV on micropatterned linear arrays of its host cells.

MATERIALS AND METHODS

Microcontact Printing

Production of stamps used in microcontact printing through photolithographic processes has been described previously (Chen et al., 1998; Kane et al., 1999). Microcontact printing substrates, 22-mm glass cover slips (Corning No. 2) or glass microscope slides (Fisher Scientific, Itasca, IL), were cleaned in piranha solution at 80°C for 30 min and rinsed for at least 2 min in ultrapure water (deionized water, >18.2 mΩ·cm resistivity). They were then dried with nitrogen and baked at 120°C for 12 to 48 h. Optically transparent thin films of titanium (50-Å thickness) and gold (100-Å thickness) were evaporated onto the coverslips.

Stamping was as described previously (Dike et al., 1999), except a 2 m*M* solution of hexa(ethylene glycol)-terminated alkanethiol [$HS(CH_2)_{11}(OCH_2CH_2)_6OCH_3$] in ethanol was used instead of a tri(ethylene glycol)-terminated alkanethiol.

Cell Seeding Onto Micropatterned Substrates

The patterned coverslips were treated with a solution of 25 μg of fibronectin per milliliter of solution in sterile phosphate-buffered saline (PBS; Sigma, St. Louis, MO) at room temperature for 2 h. They were then rinsed twice with 75 mL of sterile PBS and placed into six-well plates containing 2 mL of serum-free culture medium prior to cell seeding. Cells were harvested, resuspended in growth medium containing 10% serum, and seeded at a concentration of 5×10^5 cells/well in 2-mL volumes. All cell culture conditions were as described previously (Duca et al., 2001).

Infection of Baby Hamster Kidney (BHK) Cells With VSV

Methods of rinsing samples and applying the agarose overlay were as described previously (Duca et al., 2001). Infections of BHK cells with VSV were initiated by introducing virus to the unpatterned cell reservoirs directly adjacent to the patterned cell arrays. A plug of agarose approximately the size of the unpatterned area (15 mm × 5 mm) along the beginning of the patterned lines was removed to form a small virus deposition reservoir. A concentrated stock of vesicular stomatitis virus (VSV-Indiana serotype, Mudd–Summers strain) as cell culture supernatant at 5×10^9 pfu/mL was diluted in infection medium to the desired concentration of 5×10^7 pfu/mL. Each well received 30 μL of virus solution. Plates remained in the incubator until the times designated for fixation. Fixation was as previously described (Duca et al., 2001).

Visualization of Viral and Cellular Markers by Immunocytochemistry

Virus propagation into the patterned cells was monitored by staining for the presence of the VSV envelope surface glycoprotein (G protein). Staining techniques were performed as previously described (Duca et al., 2001), except for the use of equine serum (Hyclone, Inc.) for the first blocking rinse, and donkey serum (Jackson ImmunoResearch, West Grove, PA) for the second blocking rinse to prevent nonspecific antibody binding. After labeling was completed, samples were stored at 4°C in a solution of PBS or PBS/0.01% sodium azide, or mounted onto microscope slides with ProLong Antifade Mounting Kit (Molecular Probes, Inc.)

Image Collection, Processing, and Analysis of Patterned Surfaces

All image collection and processing was performed as described previously (Duca et al., 2001). Measurements of propagation distance were made using SCIONIMAGE v1.62a (National Institutes of Health). The propagation distance was directly measured manually from the point of infection initiation to the leading edge of the infection. The average propagation velocity was determined by linear regression of the distance per time data. Although uncertainty was introduced by the manual determination of the infected distance endpoint, the variability in distance measurements among different times of measurement was <2%, which is considerably less than the variation in replicate measurements. These measurements were also verified by determining the plot profiles of selected lines, using the plot profile command in SCIONIMAGE. The maximum percent difference between manual measurements versus using the profile method was <4%, which is also less than the variation in replicate measurements of propagation distance.

RESULTS AND DISCUSSION

Using Microcontact Printing to Pattern Substrates and BHK Host Cells

Control over the in vitro spread of virus can be facilitated by supplying spatially contiguous, susceptible host cells along the desired direction of propagation. Baby hamster kidney-21 (BHK-21) cells were patterned in arrays of various widths (40, 80, and 140 μm; Fig. 1) separated by uniform nonadhesive spacings of 100 μm. Although cells were slightly elongated along line boundaries, we saw no detrimental effects of the patterning on cell viability. The few poorly adhered cells that were visible within the lines appeared to result from cell division, whereas those cells located in the cell-resistant regions were rounded due to the lack of adhesive area available for cell attachment.

Determination of Characteristic Velocity Profiles

VSV G protein is visible in locations where intact virions or free G protein is present. Because the infection was localized along the beginning of the lanes, the viruses were forced to spread from cell to cell. In the unpatterned assay, cells are plated into multiwell tissue culture polystyrene plates, the infection is initiated in the center of the cell monolayer, and the virus then spreads from cell to cell in a radial fashion. The propagation distance of VSV G protein is shown (Fig. 2a and b) in two patterned samples of cells fixed and stained for the VSV G protein at 12 and 36 h postinfection, respectively. If several lane arrays are fixed at different postinfection timepoints, a characteristic viral propagation velocity can be determined by taking the slope of the propagation distance versus time postinfection.

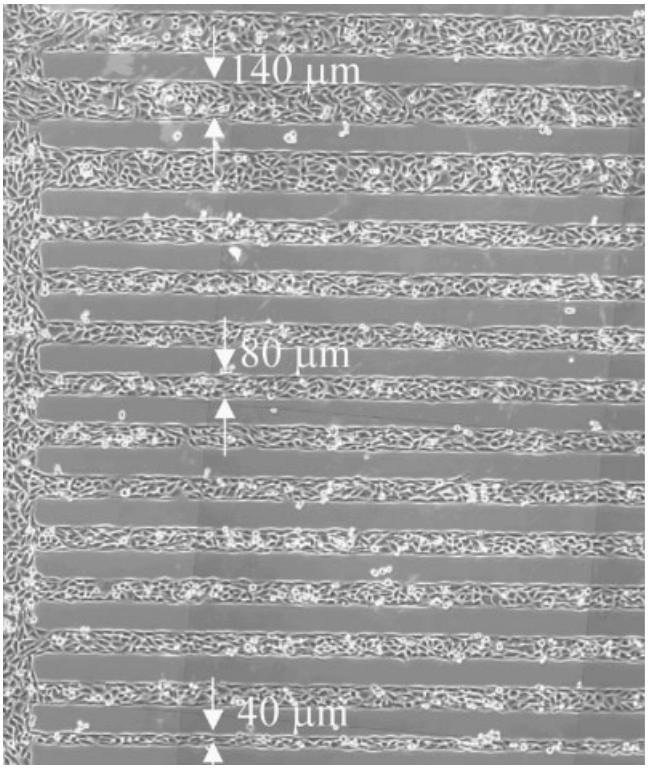

Figure 1. BHK cells patterned in 140-μm, 80-μm, and 40-μm-wide lines, separated by 100-μm spaces, at 19 h postplating. Part of the unpatterned reservoir can be seen at the far left of the image.

We found that VSV spread with a roughly constant rate in both patterned and unpatterned host cells, as reflected by the 45 ± 1.3 μm/h and 54 ± 3.5 μm/h velocities of propagation, respectively (Fig. 3). Student's *t*-test was used to compare the mean propagation velocities between patterned and unpatterned samples. The probability that the two means are not different is 0.0176; at the 95% significance level, these velocities are statistically significant from one another. The difference in viral propagation between patterned and unpatterned samples may arise from differences in the geometry of spread, or differences in the interactions of the host cells or viruses with the underlying surface chemistry, issues that are currently under investigation.

The viral spread was not due to simple diffusion of the initial virus inoculum. If free diffusion were the dominant mode of viral propagation, the propagation distance would

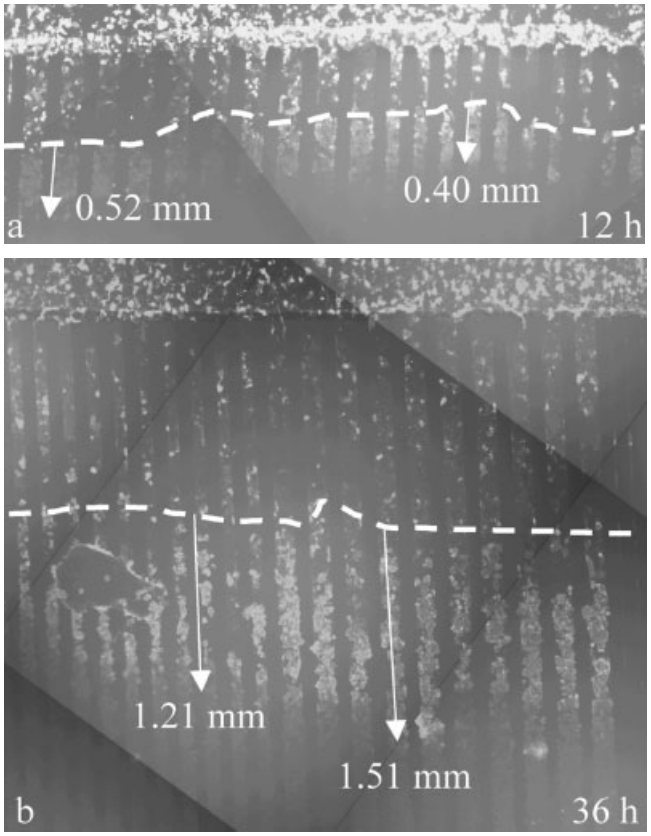

Figure 2. VSV infection in patterned BHK-21 cells. Propagation distances are shown at (a) 12 h and (b) 36 h postinfection. The dashed line indicates the boundary above which the infection was initiated. Arrows at each timepoint indicate measured viral propagation distances based on detection of immunofluorescently labeled viral G protein.

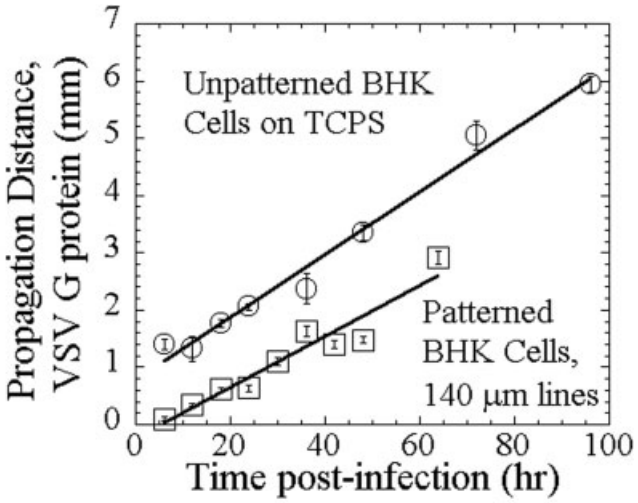

Figure 3. Propagation profiles of VSV in patterned and unpatterned BHK cells show similar trends. Monolayers of BHK cells were cultured on each surface for approximately 16 h prior to infection. The propagation rates were found to be 55 μm/h and 44 μm/h for corresponding unpatterned and patterned cells, respectively. The average propagation rate was taken as the slope of the best-fit line to the data, with linear correlation coefficients of 0.99156 and 0.96195 for unpatterned BHK cells on TCPS and 140-μm lines, respectively. Data points represent the mean area equivalent radius ± the standard error of the mean. The propagation distance in unpatterned BHK cells on TCPS was determined by measuring the total infected area in a sample and calculating a radius from this area (six samples per point). The propagation distance in patterned cells (20 to 40 samples per point) was measured linearly from the starting point of the infection at the beginning of the lines to the end of the infection within the line, as denoted by the change in fluorescence.

be expected to depend on $(\text{time})^{1/2}$ instead of the observed linear dependence on time. The exact propagation velocities from the two surfaces must be compared with care, as the radial spread of virus in traditional (unpatterned) cell culture systems uses a different method to calculate the average propagation distance (Duca et al., 2001). Moreover, the geometry of the two systems may permit viruses produced in unpatterned cells to adsorb to greater numbers of nearest-neighbor host cells than viruses replicating in patterned cells. The viability of the cells on these surfaces remained high (>85%, as determined by trypan blue exclusion) throughout the time course of these experiments.

The observed linear trend of propagation velocity was also independent of the line widths for line widths of 40, 80, and 140 μm (Fig. 4). Apparent drops in propagation distance can arise as the time postinfection increases (Fig. 3), because multiple samples are needed to generate each propagation curve. Thus, this drop in propagation distance does not indicate that the viral front is regressing, but rather that plate-to-plate variation exists between samples. To label the viral surface protein, the samples must be chemically fixed, stopping propagation at each postinfection timepoint. A way to address this challenge is to track viral propagation in real time by monitoring a single infected sample throughout the entire course of the experiment using recombinant VSV constructs that contain the gene that encodes the production of green fluorescent protein (GFP). Viral propagation can be tracked as propagation progresses, as GFP is produced along with viral proteins, and the presence of GFP does not compromise the ability of VSV to infect BHK cells (Boritz et al., 1999; Stillman and Whitt, 1999).

Spatial Resolution of Different Stages of Infections

As a viral infection spreads, its leading edge continuously initiates new infections in receptive host cells. Trailing back from the leading edge, the host cells exist at many different stages of infection. Figure 5a illustrates the boundary between infected and uninfected cells at the leading edge of the propagation front and shows that the viral front was seen in advance of the cytopathic effect. In the uninfected cells, the individual cell nuclei were distinctly visible, and there was no viral marker visible. In the cells that were recently infected, directly to the left of the uninfected cells, distinct nuclei were still visible, but the G protein was colocalized with the nuclei. There was no cell damage visible by phase-contrast at this stage of infection. Relative to Figure 5a, Figure 5b shows a more advanced stage of infection. Significant nuclear changes became apparent, and cell nuclei

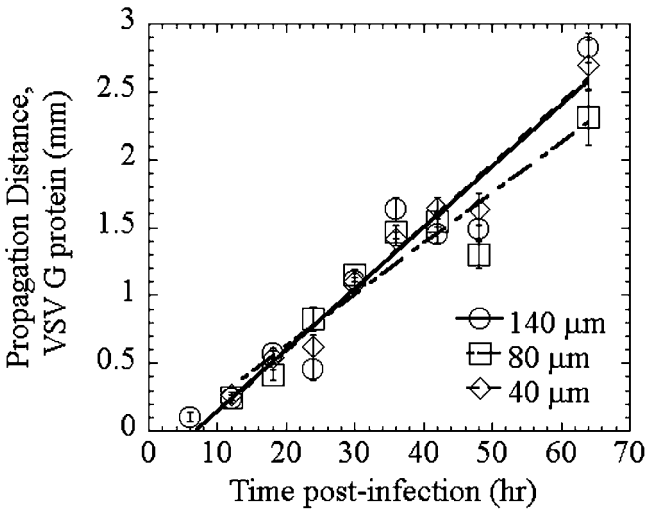

Figure 4. Line width differences do not result in differences in the propagation of VSV in patterned BHK cells. Monolayers of BHK cells were cultured on the surface for approximately 16 h prior to infection. The propagation rates of VSV on 140-μm, 80-μm, and 40-μm lines were calculated to be 45 μm/h, 37 μm/h, and 46 μm/h, respectively. The average propagation rate was taken as the slope of the best-fit line to the data, with linear correlation coefficients of 0.96195, 0.95737, and 0.98747 for 140-μm, 80-μm, and 40-μm lines, respectively. Data points represent the mean area equivalent radius ± the standard error of the mean of 20 to 40 samples per point.

and viral protein were colocalized. Organized nuclear structures are common indicators of cell fusion, and they can take many geometric forms ranging from tightly packed, elongated rows of nuclei to the ring structures seen here (Holmes and Choppin, 1968; Wang et al., 1979). Many viruses are fusogenic and are capable of inducing cell fusion and nuclear rearrangement (Holmes and Choppin, 1968; Wang et al., 1979). These rings are formed by the movement of nuclei from several cells into the fused cell body through many elements of the cytoskeleton, including microtubules and 10-nm intermediate filaments (Holmes and Choppin, 1968; Wang et al., 1979, 1981). VSV is capable of inducing cell fusion, typically in a low pH-dependent manner. Figure 5c shows few visible nuclei; by this time, most cells were infected and had suffered severe, virus-induced cytopathic effects. The disorganization of the nuclear ring formations (Fig. 5c) would be consistent with the interaction of the matrix protein, or M protein, with tubulin, as this interaction is believed to be the underlying cause of the microtubule disorganization (Melki et al., 1994). In culture, such interactions normally initiate cytoskeletal reorganization and, in BHK cells, cause cells to round (Blondel et al., 1990; Melki et al., 1994) and detach from tissue culture surfaces. As shown in Figure 5d, the nuclear label was no longer visible, consistent with an infection stage where cells had detached from the surface. The leading edge of this bare area was characterized as the death front, or the final cytopathic effect that resulted from viral infection.

Applications and Implications for Technology

The integration of microcontact printing and immunofluorescence microscopy has enabled the development of a new technique that describes the infection process in a specific virus–host system through the viral propagation velocity. The advantages to using the patterned surfaces to characterize the dynamics of viruses and their host cells are fourfold. First, the patterned surfaces offer greater potential control over the molecular level structure of the cell substrate than tissue culture polystyrene. The control introduced by self-assembled monolayers has enabled previous investigations of biospecific, molecular interactions between cells and surfaces (Franco et al., 2000; Lewandowska et al., 1992; Mrksich, 2000). The importance of surface interactions with host cells during viral infections is illustrated by the ability of weakly adherent cells to present the viral glycoprotein on the cell surface, in contrast to strongly adherent cells, which instead secrete the glycoproteins (Kabat et al., 1985). Because of the reliance of viruses on host cell resources, it is quite likely that controlled surfaces will impact the study of viruses through additional effects exerted on host cells.

Second, the control of geometries also lends itself well to the testing of cellular mechanisms that are involved in viral spread. In many viral systems, the use of the cellular structural filaments is key in releasing virions from the cell (Sodeik, 2000). By using SAMs, we can control the direction and alignment of the cells, which may enable us to increase our understanding of the underlying structural mechanisms that affect the efficiency of viral spread. Cells typically exhibit orientation or direction in their native environments, and this orientation can play a significant role in virus propagation. For example, influenza virus and VSV exhibit

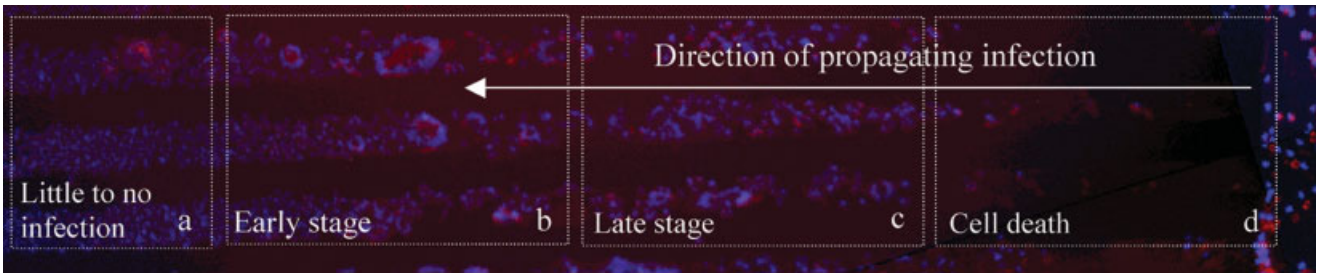

Figure 5. Spatial resolution of dynamic changes in cell morphology following viral infection of patterned cells. The virus infection front was initiated at the far right edge and gradually propagated to the left along the patterned cell arrays. Different temporal stages of infection were visible at different locations along the arrays. The arrays were 80 μm wide and the sample was fixed for staining at 42 h postinfection.

opposite trafficking patterns in polarized epithelial cells, such as MDCK cells. Influenza exits through the apical domain, whereas VSV exits through the basolateral domain (Flint et al., 2000).

Third, patterned cell arrays provide an opportunity to track different virus populations in a controlled environment. When an infection is initiated with a roughly clonal viral population, the directionality of the host cells may allow the emergence of fast-growing mutations to be identified within the virus populations confined in separate lines. Also, if multiple virus populations are present in separate lines on the array, they may each have dramatically varied susceptibilities to an antiviral agent that is added uniformly to the sample.

Finally, because infections in each line may be initiated independently of one another, many parallel "experiments" can be performed within a single multiline sample. This parallelism eliminates much of the materials and labor required to perform these experiments in cells on traditional surfaces, and also helps to minimize the experimental variations that occur due to differences between samples. For example, here the use of patterned surfaces has allowed us to increase by 10- to 20-fold the number of replicates per cell substrate, reducing up to 33-fold the amount of antibody needed per measured propagation distance. However, a key point of this assay is that the patterns are maintained such that the lines remain independent of one another. The array patterns remained defined throughout the course of the experiment, up to approximately 90 h after the cells were initially plated. When samples were stained for the presence of viral protein and cell nuclei, no evidence was found that would suggest cells or viral proteins were present outside of the initial patterned area for cell adhesion. It has been shown in the literature that cellular patterns of fibroblasts can be maintained in culture for up to 7 days (Luk et al., 2000). However, to study this system over a longer time period, SAMs containing protein-resistant groups more effective than oligo(ethylene glycol), such as mannitol (Luk et al., 2000), may support the development of this technique as a screening and characterization tool for virus–host cell systems.

We seek to complement and enrich methods to characterize the intra- and extracellular dynamics of viral infections. Currently, in vivo methods provide the most natural host-cell context for investigating viral propagation and host innate and adaptive immune responses to infection, but they are material- and labor-intensive to implement, because it is difficult to monitor individual processes when only the final disease state can be observed. Alternatively, in vitro methods often focus on single viral replication cycles and specific molecular details, with less attention given to the host-cell context and its potential effect on the cell–virus dynamics. We have begun to incorporate desirable features of both in vivo and in vitro methods by propagating viral infections on patterned cells. Self-assembled monolayers have enabled us to control cell placement and geometry while retaining the accessibility of viral mechanisms and cellular responses to probing by in vitro techniques.

A long-term goal of tissue engineering is to create environments that enable cultured cells to closely mimic the in vivo structure and function of tissues. Advances in understanding how physical, chemical, and biological cues in the extracellular environment influence cell behavior will improve our ability to create more in vivo-like virus culture systems. Such systems will support the evaluation of antiviral agents and contribute to the development of improved strategies for treating viral disease.

The authors thank Michelle Arnold, Vy Lam, Jaz Bansel, and Rahul Shah, as well as the research group of Prof. Nicholas Abbott, for their invaluable technical contributions to this work.

References

Beijerinck MW. 1898. Over een Contagium vivum fluidum als oorzak van de Vlekziete der tabaksbladen. Versl Gewone Vergad Wis- Natuurkd Afd, K Akad Wet Amsterdam 7:229–235.

Block TM, Deshmane S, Masonis J, Maggioncalda J, Valyi-Nagi T, Fraser NW. 1993. An HSV LAT null mutant reactivates slowly from latent infection and makes small plaques on CV-1 monolayers. Virology 192:618–630.

Blondel D, Harmison GG, Schubert M. 1990. Role of matrix protein in cytopathogenesis of vesicular stomatitis virus. J Virol 64:1716–1725.

Boritz E, Gerlach J, Johnson JE, Rose JK. 1999. Replication-competent rhabdoviruses with human immunodeficiency virus type 1 coats and green fluorescent protein: Entry by a pH-independent pathway. J Virol 73:6937–6945.

Chen CS, Mrksich M, Huang S, Whitesides GM, Ingber DE. 1997. Geometric control of cell life and death. Science 276:1425–1428.

Chen CS, Mrksich M, Huang S, Whitesides GM, Ingber DE. 1998. Micropatterned surfaces for control of cell shape, position, and function. Biotechnol Progr 14:356–363.

Cooper PD. 1961. The plaque assay of animal viruses. In: Smith KM, Lauffer MA, editors. Advances in virus research. New York: Academic Press. p 319–378.

Dallo S, Rodriguez JF, Esteban M. 1987. A 14K Envelope protein of vaccinia virus with an important role in virus-host cell interactions is altered during virus persistence and determines the plaque size phenotype of the virus. Virology 159:423–432.

d'Herelle FCR. 1917. Sur un microbe invisible antagoniste des bacillus dysenteriques. CR Acad Sci Ser D 165:373.

Dike LE, Chen CS, Mrksich M, Tien J, Whitesides GM, Ingber DE. 1999. Geometric control of switching between growth, apoptosis, and differentiation during angiogenesis using micropatterned substrates. In Vitro Cell Dev Biol Anim 35:441–448.

Duca KA, Lam V, Keren I, Endler EE, Letchworth GJ, Novella IS, Yin J. 2001. Quantifying viral propagation *in vitro*: Toward a method for characterization of complex phenotypes. Biotechnol Progr 17:1156–1165.

Dulbecco R. 1952. Production of plaques in monolayer tissue cultures by single particles of an animal virus. Proc Natl Acad Sci USA 38: 747–752.

Flint SJ, Enquist LW, Krug RM, Racaniello VR, Skalka AM, editors. 2000. Principles of virology: Molecular biology, pathogenesis, and control. Washington, DC: ASM Press.

Franco M, Nealy PF, Campbell S, Teixeira AI, Murphy CJ. 2000. Adhesion and proliferation of corneal epithelial cells on self-assembled monolayers. J Biomed Mater Res 52:261–269.

Gong S, Lai C, Dallo S, Esteban M. 1989. A single point mutation of Ala-25 to Asp in the 14,000-M_r envelope protein of vaccinia virus

induces a size change that leads to the small plaque size phenotype of the virus. J Virol 63:4507–4514.
Healy KE, Thomas CH, Rezania A, Kim JE, McKeown PJ, Lom B, Hockberger PE. 1996. Kinetics of bone cell organization and mineralization on materials with patterned surface chemistry. Biomaterials 17:195–208.
Holmes KV, Choppin PW. 1968. On the role of microtubules in movement and alignment of nuclei in virus-induced syncytia. J Cell Biol 39:526–543.
Iizuka N, Kohara M, Hagino-Yamagishi K, Abe S, Komatsu T, Tago K, Arita M, Nomoto A. 1989. Construction of less neurovirulent polioviruses by introducing deletions into the 5′ noncoding sequence of the genome. J Virol 63:5354–5363.
Iyer VR, Eisen MB, Ross DT, Schuler G, Moore T, Lee JCF, Trent JM, Staut LM, Hudson J, Boguski MS, Lashkari D, Shalon D, Botstein D, Brown PO. 1999. The transcriptional program in the response of human fibroblasts to serum. Science 283:83–87.
Kabat D, Gliniak B, Rohrschneider L, Polonoff E. 1985. Cell anchorage determines whether mammary tumor virus glycoproteins are processed for plasma membranes or secretion. J Cell Biol 101:2274–2283.
Kane RS, Takayama S, Ostuni E, Ingber DE, Whitesides GM. 1999. Patterning proteins and cells using soft lithography. Biomaterials 20: 2363–2376.
Lee Y, Yin J. 1996. Detection of evolving viruses. Nat Biotechnol 14: 491–493.
Lewandowska K, Pergament E, Sukenik CN, Culp LA. 1992. Cell-type - specific adhesion mechanisms mediated by fibronectin adsorbed to chemically derivatized substrata. J Biomed Mater Res 26:1343–1363.
Luk Y-Y, Kato M, Mrksich M. 2000. Self-assembled monolayers of alkanethiolates presenting mannitol groups are inert to protein adsorption and cell attachment. Langmuir 16:9604–9608.
Melki R, Gaudin Y, Blondel D. 1994. Interaction between tubulin and the viral matrix protein of vesicular stomatitis virus: Possible implications in the viral cytopathic effect. Virology 202:339–347.
Mrksich M. 2000. A surface chemistry approach to studying cell adhesion. Chem Soc Rev 29:267–273.
Ostuni E, Yan L, Whitesides GM. 1999. The interaction of proteins and cells with self-assembled monolayers of alkanethiolates on gold and silver. Coll Surf. B Biointerf 15:3–30.
Rose JK, Whitt MA. 2001. *Rhabdoviridae:* The viruses and their replication. In: Straus SE, editor. Fields virology. Philadelphia: Lippincott–Williams & Wilkins. p 1221–1244.
Sambrook J, Fritsch EF, Maniatis T, editors. 1989. Molecular cloning: A laboratory manual. Cold Spring Harbor, NY: Cold Spring Harbor Laboratory.
Sodeik B. 2000. Mechanisms of viral transport in the cytoskeleton. Trends Microbiol 8:465–472.
Steele JG, Dalton BA, Johnson G, Underwood PA. 1995. Adsorption of fibronectin and vitronectin onto Primaria™ and tissue culture polystyrene and relationship to the mechanism of initial attachment of human vein endothelial cells and BHK-21 fibroblasts. Biomaterials 16:1057–1067.
Stillman EA, Whitt MA. 1999. Transcription initiation and 5′-end modifications are separable events during vesicular stomatitis virus transcription. J Virol 73:7199–7209.
Terramani TT, Eton D, Bui PA, Wang Y, Weaver FA, Yu H. 2000. Human macrovascula endothelial cells: Optimization of culture conditions. In Vitro Cell Dev Biol Anim 36:125–132.
Twort FW. 1915. An investigation on the nature of the ultra-microscopic viruses. Lancet ii:1241–1245.
Wang E, Cross RK, Choppin PW. 1979. Involvement of microtubules and 10-nm filaments in the movement and positioning of nuclei in syncytia. J Cell Biol 83:320–337.
Wang E, Roos DS, Heggeness MH, Choppin PW. 1981. Function of cytoplasmic fibers in syncytia. Cold Spring Harb Symp Quant Biol 46: 997–1012.
Yin J. 1993. Evolution of bacteriophage T7 in a growing plaque. J Bacteriol 175:1272–1277.
Yin J, McCaskill JS. 1992. Replication of viruses in a growing plaque: A reaction–diffusion model. Biophys J 61:1540–1549.
You LC, Yin J. 1999. Amplification and spread of viruses in a growing plaque. J Theor Biol 200:365–373.